A R C H I V E S O F M E T A L L U R G Y A N D M A T E R I A L S
Volume 58 2013 Issue 4
DOI: 10.2478/amm-2013-0144

E. ROŻNIATA*

THE MICROSTRUCTURES AND ENERGY DISPERSIVE SPECTROSCOPY ANALYSIS OF A HYPOEUTECTOID STEELS WITH 1% Cr

ANALIZA MIKROSTRUKTURY I EDS STALI PODEUTEKTOIDALNYCH Z 1% CHROMU

The results of a microstructure, Energy Dispersive Spectroscopy analysis and hardness investigations of the hypoeutectoid steels with 1% Cr, imitating by its chemical composition toughening steels, are presented in the paper.

Dilatometric tests were performed using L78R.I.T.A dilatometer of the German company LINSEIS. Using dilatometer the changes of elongation (Δl) of the samples with dimensions φ 3X10mm as a function of temperature (T) were registered. Obtained heating curves were used to precisely determine the critical temperatures (critical points) for the tested steels, while the differentiation of obtained cooling curves allowed to precisely define the temperatures of the beginning and the end of particular transition to draw two CCT diagrams.

The analysis of the chemical composition of the phases present in the studied steels for different cooling rates were performed using an electron microprobe (X-ray microanalyzer). In this study a point, linear and a fixed area analysis techniques were used. After placing the samples tested steels in the chamber and the achievement of appropriate vacuum, spots for analysis were identified and the EDS analysis (Energy Dispersive Spectroscopy) was performed. EDS analyzes were performed using Nova NanoSEM 450 scanning electron transmission microscope.

Developed CCT diagrams in accordance with the Rose and Wever classification are of type IV, which means that the diffusional transformations are separated by a stability range of the undercooled austenite and have the shape of the letter ”C”. The hardenability of tested steels is similar, but molybdenum acts much more effectively than nickel. Molybdenum occupies the I-st place among the effectiveness of alloying elements for the steels designed for low tempering, where the ”background” of other elements is weak. For both tested hypoeutectoid steels an EDS analysis revealed the precipitation of alloyed cementite at the grain boundaries. Chromium, as a ferrite creative element, quite strongly diffuses into the grain boundaries. It is visible with the change of chromium distribution along pearlite/ferrite grains boundaries.

Keywords: microstructure, EDS analysis, CCT diagram, heat treatment, hypoeutectoid steel

W artykule zamieszczono wyniki badań mikrostruktury, analizy EDS i twardości stali podeutektoidalnych z 1% Cr imitujących składem chemicznym stale do ulepszania cieplnego.

Badania dylatometryczne wykonano przy użyciu dylatometru L78R.I.T.A niemieckiej firmy LINSEIS. Za pomocą dylatometru rejestrowano zmiany wydłużenia (Δl) próbek o wymiarach φ 3X10mm w funkcji temperatury (T). Otrzymane krzywe nagrzewania posłużyły do precyzyjnego wyznaczenia temperatur krytycznych (punktów przełomowych) dla badanych stali. Natomiast otrzymane krzywe chłodzenia różniczkowano, co pozwoliło precyzyjnie określić temperatury początków i końców poszczególnych przemian dla wykonania dwóch wykresów CTPc.

Analizę składu chemicznego występujących faz w badanych stalach dla różnych szybkości chłodzenia wykonano przy użyciu mikrosondy elektronowej (mikroanalizator rentgenowski).

W niniejszej pracy wykorzystano technikę analizy punktowej, liniowej oraz w obszarze o ustalonym polu. Po umieszczeniu próbek z badanych stali w komorze i osiągnięciu odpowiedniej próżni, wyszukano miejsca i dokonano analizy techniką EDS (Energy Dispersive Spectroscopy). Analizy EDS dokonano przy użyciu skaningowego mikroskopu transmisyjnego typu Nova NanoSEM 450.

Opracowane wykresy CTPc zgodnie z klasyfikacją Wever'a i Rose'go są typu IV, co oznacza, że przemiany dyfuzyjne są rozdzielone zakresem trwałości przechłodzonego austenitu i mają kształt litery „C”. Hartowność badanych stali jest zbliżona, jednak molibden działa zdecydowanie skuteczniej niż nikiel. Molibden zajmuje I-sze miejsce wśród skuteczności pierwiastków stopowych dla stali do niskiego odpuszczania, gdzie „tło” pierwiastków jest słabe. Dla obu badanych stali podeutektoidalnych analiza EDS wykazała wydzielanie się cementytu stopowego na granicach ziaren. Chrom, jako pierwiastek ferrytotwórczy dość silnie dyfunduje do granic ziaren. Widocznie jest to przy zmianie rozkładu chromu na graniach ziaren perlit/ferryt.

* AGH UNIVERSITY OF SCIENCE AND TECHNOLOGY, FACULTY OF METALS ENGINEERING AND INDUSTRIAL COMPUTER SCIENCE, AL. A. MICKIEWICZA 30, 30-059 KRAKOW, POLAND

1. Introduction

Good mechanical properties of hypoeutectoid and hypereutectoid steels are achieved by their chemical composition and the microstructure obtained by appropriately designed heat treatment [1÷7]. Therefore, these steels should have a suitably complex chemical composition, carbon content from 0.35% to 0.40% and the specific kinetics of phase transformation of undercooled austenite [8÷13]. These alloys represent large groups of alloy steels designated for quenching and tempering, which are subjected to high requirements regarding R_e/R_m ratio as well as ductility and toughness.

The analysis of microgradients of chemical compositions seems to be important for these alloys. It should be noted that the interaction of two or more alloying elements is significantly different from the sum of effects of these elements added separately. The most important may be the common effect of molybdenum and chromium, molybdenum and nickel, chromium and nickel, manganese and chromium, manganese and nickel, manganese and molybdenum, manganese and cobalt. This mutual interaction of various elements on the effects of the others, may be the basis for among others assessment of the impact magnitude of each of them on e.g. hardenability of steel in the conditions of the presence of even one or several other elements in the above mentioned alloys with iron matrix. Until now, the impact of each element was considered separately, only sometimes, pointing to a group of alloys, in which this interaction was evaluated.

2. Research material

The material for study were two hypoeutectoid steels: 38MnCrNi6-4-4 and 39MnCrMo6-4-3 (marked in accordance with PN-EN10027-1:1994 standard). Steels in the form of model alloys were supplied as cast by Z. J. Głuchowski S. C. Kooperacja Przemysłowo-Handlowa in Gliwice, and then were reforged in INTECH-MET S. C. plant in Gliwice.

Chemical compositions of tested steels are shown in Table 1.

TABLE 1
Chemical compositions of tested hypoeutectoid steels, % by mass

No.	Steel Symbol	C	Mn	Cr	Ni	Mo	Si	Al	P
1	38MnCrNi6-4-4	0.38	1.56	1.10	0.98	-	0.09	-	0.001
2	39MnCrMo6-4-3	0.39	1.58	1.02	-	0.28	0.09	0.01	0.001

Both tested steels are hypoeutectoid with a carbon content of about 0.4% and similar content of manganese and chromium. They differ in the content of alloying elements such as nickel and molybdenum. The microstructures of tested steels in the state after forging is shown in Figure 1.

As can be seen both steels in a state after forging have pearlite-ferritic microstructure, but they differ in morphology. There is a ferrite present on grain boundaries of the former austenite in steel containing 1% of Ni, forming a grid. The microstructure of steel with 0.3% Mo has a ferrite in Widmannstätten system. It is known from the literature that in hypoeutectoid steels the Widmannstätten structure is characterized by the parallel plates (needles) of ferrite which intersect at an angle of 60° and 120°.

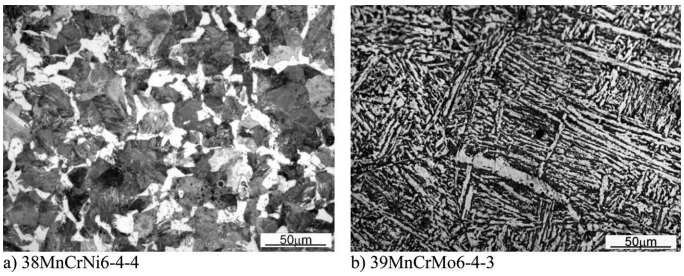

a) 38MnCrNi6-4-4 b) 39MnCrMo6-4-3

Fig. 1. The microstructures of hypoeutectoid steels in after forging state

In order to determine the correct critical temperatures (critical points) for both tested steels after forging the sample were heated at the rate of 0.05°C/s to a temperature of 1100°C and then cooled at the rate of 1°C/s to room temperature. Critical temperatures read are shown in Table 2.

TABLE 2
Critical temperatures determined for both hypoeutectoid steels in a state after forging

No.	Steel	Ac_{1s}	Ac_{1f}	Ac_3
1	38MnCrNi6-4-4	720°C	750°C	780°C
2	39MnCrMo6-4-3	740°C	765°C	820°C

Temperatures of critical points confirm the behavior of both alloying elements in the studied steels. Nickel, as an austenite creative element lowers the critical temperatures, whereas molybdenum, which is highly ferrite creative significantly shifts the critical temperatures upward. The biggest difference can be seen at a temperature Ac_3, which is 40°C.

3. Experimental procedure

The chemical composition of the model alloy was designed in the Laboratory of Phase Transformations, Department of Physical and Powder Metallurgy, AGH University of Science and Technology.

The microstructure of the investigated material was examined using the light microscope Axiovert 200 MAT.

The hardness measurements were performed with the Vickers HPO250 apparatus.

The dilatometric measurements were performed with the L78R.I.T.A. dilatometer.

EDS analyzes were performed using Nova NanoSEM 450 scanning electron transmission microscope at the Faculty of Metals Engineering and Industrial Computer Science at the Department of Surface Engineering and Materials Analyzes.

4. Results and discussion

4.1. Heat treatment (full annealing)

In order to obtain a microstructure similar to the equilibrium state the full annealing was performed for the tested 38MnCrNi6-4-4 and 39MnCrMo6-4-3 steels. After such annealing the necessary treatment for mechanical testing and to remove the internal stress and improve the workability is easier to perform.

Full annealing was performed in a Carbolite RHF 16/19 laboratory oven. Samples were heated to a temperature by 50°C higher than the Ac_3 for test steels, maintained at this temperature for 2 hours and then cooled at the rate of 3°C/min to a temperature of 500°C and further at the rate of 30°C/min to room temperature. The microstructures of both steels in state after full annealing are shown in Figure 2.

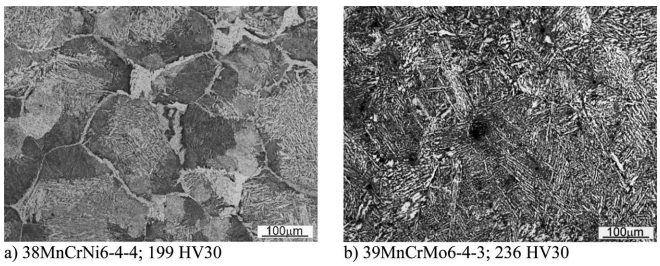

a) 38MnCrNi6-4-4; 199 HV30 b) 39MnCrMo6-4-3; 236 HV30

Fig. 2. Microstructures of hypoeutectoid steels after full annealing

The microstructure of the 38MnCrNi6-4-4 steel with nickel consists of large grains of pearlite surrounded by ferrite grid. There is needle shaped ferrite in Widmannstätten system present inside of austenite grains. Ferrite in some places along grain boundaries has the needle type nature (compare Fig. 2a).

The microstructure of 39MnCrMo6-4-3 steel with molybdenum is not significantly different when compared with the microstructure in state after forging. The microstructure of this steel is composed of ferrite in Widmannstätten system. The only difference is the size of austenite grains, which in this case is considerably greater. Grain boundaries are not as evident as in case of steel with nickel.

After full annealing the critical points of tested steels were determined for the second time. The treatment parameters were the same as before - both steels were heated at a rate of 0.05°C/s up to a temperature of 1100°C, and then cooled at a rate of 1°C/s to room temperature. An example of dilatometric curve, from which the critical temperatures were read, is presented in Figure 3 for 38MnCrNi6-4-4 steel.

The critical temperatures determined for tested steels are presented in Table 3.

The critical temperatures for 38MnCrNi6-4-4 steel did not change, whereas in case of 39MnCrMo6-4-3 steel they are different when compared with the state after forging. The Ac_1 temperature range has been considerably extended: both for Ac_{1s} (740°C → 725°C), and for Ac_{1f} (765°C → 780°C). The Ac_3 temperature of steel with molybdenum is greater by 20°C, while the Ac_3 temperatures difference between the steels is 60°C.

TABLE 3
Critical temperatures determined for both hypoeutectoid steels in state after full annealing

No.	Steel	Ac_{1s}	Ac_{1f}	Ac_3
1	38MnCrNi6-4-4	720°C	750°C	780°C
2	39MnCrMo6-4-3	725°C	780°C	840°C

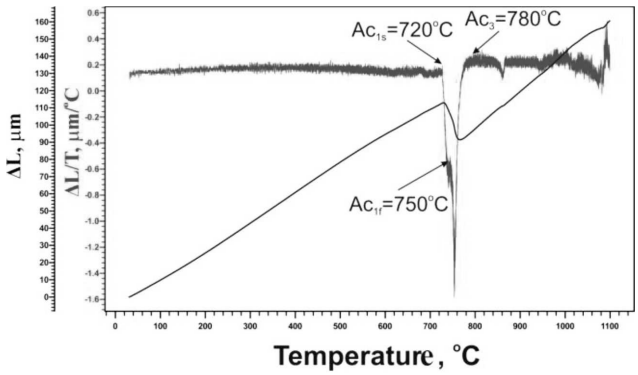

Fig. 3. Heating curve of 38MnCrNi6-4-4 steel after full annealing up to the temperature of 1100°C and the corresponding differential curve with marked critical points

4.2. Analysis of the kinetics of undercooled austenite phase transformations

On the basis of determined critical temperatures of both steels hypoeutectoid austenitizing temperatures were chosen and the kinetics of undercooled austenite was analyzed. The austenitizing temperature was assumed 50°C higher than Ac_3 critical temperature of each of the tested steels. Samples of steels, both with molybdenum and nickel, were cooled at 6 different rates from the austenitizing temperature within different ranges (for 38MnCrNi6-4-4 steel 25÷0.33°C/s, and for 39MnCrMo6-4-3 steel in the range 50÷0.16°C/s). Then the temperatures of beginnings and ends of each transformation was read from obtained dilatometric curves. An example of dilatometric curve for 38MnCrMo6-4-3 steel is presented in Figure 4.

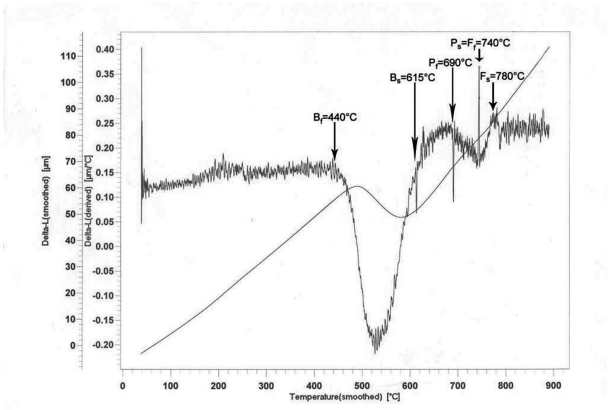

Fig. 4. Dilatometric curve of cooling the sample form the austenitizing temperature T_A = 890°C with corresponding differential curve, with marked start and finish temperatures of phase transformations

4.3. CCT diagram for 38MnCrNi6-4-4 and 39MnCrMo6-4-3 steels

Figures 5 and 6 present CCT diagrams for 38MnCrNi6-4-4 steel after austenitizing at the temperature T_A = 830°C and 39MnCrMo6-4-3 steel after austenitizing at the temperature T_A = 890°C.

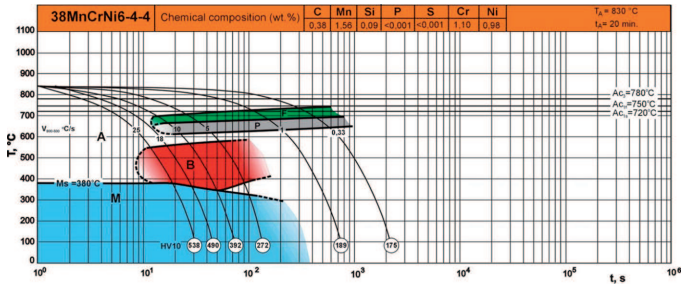

Fig. 5. The CCT diagram for 38MnCrNi6-4-4 steel after austenitizing at the temperature T_A = 830°C [14]

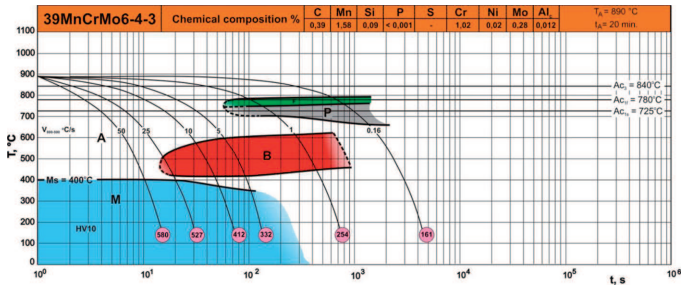

Fig. 6. The CCT diagram for 39MnCrMo6-4-3 steel after austenitizing at the temperature T_A = 890°C

Both presented diagrams in accordance with the Rose and Wever classification are of the type IV [15], because the transition ranges are separated and thus the curves of the beginning of transformations are continuous. This means that the "noses" of pearlite and ferritic transformations (diffusional transformations) converge at single point. Between the diffusional transformations and bainite transition there is a stability range of stable austenite.

For 38MnCrNi6-4-4 steel austenitized at the temperature T_A = 830°C the beginning of ferrite precipitation is observed between 25°C/s and 10°C/s cooling curves. Temperature of the beginning of martensitic transition for test steel with nickel is Ms = 380°C.

In case of 39MnCrMo6-4-3 steel, which was austenitized at T_A = 890°C, the beginning of ferrite precipitation was not observed until between 5°C/s a 1°C/s cooling curves. The bainitic transition begins, alike in case of steel with nickel, at the cooling rate of 25°C/s. The of the beginning of martensitic transition for 39MnCrMo6-4-3 test steel is Ms = 400°C.

Comparing the CCT diagrams for test steels, one may state that addition of molybdenum in amount of 0.3% increases the hardenability of steel significantly more than addition of nickel in amount of 1%. Namely, the elements forming their own carbides (among others Mo, Cr) postpone the beginning of transformation, especially diffusional ones, allowing to lower the critical cooling rate (increasing the hardenability of the steel). According to CCT diagram for steel with molybdenum (Fig. 6), the postponing time of the beginning of phase transformations is almost five times longer than in case of 38MnCrNi6-4-4 steel with nickel (compare with Fig. 5). One should note that nickel (as well as manganese) is an austenite creative element and its addition does not change the characteristics of "C" curves but only shifts them towards longer times. On both CCT diagrams of test hypoeutectoid steels one may observe separation of areas of diffusional transformation from intermediate one of super cooled austenite range. For 39MnCrMo6-4-3 steel the separation of pearlite range from bainitic one is much more broader than for 38MnCrNi6-4-4 steel. This is caused not only by the presence of 1%Cr but also the content of 0.3%Mo in the chemical composition of 39MnCrMo6-4-3 steel. Mo and Cr are ferrite creative elements, which limit the presence of γ solid solution (austenite) in iron alloys.

Figures 7 and 8 present the microstructures of dilatometric samples of both tested hypoeutectoid steels used for drawing of CCT diagrams.

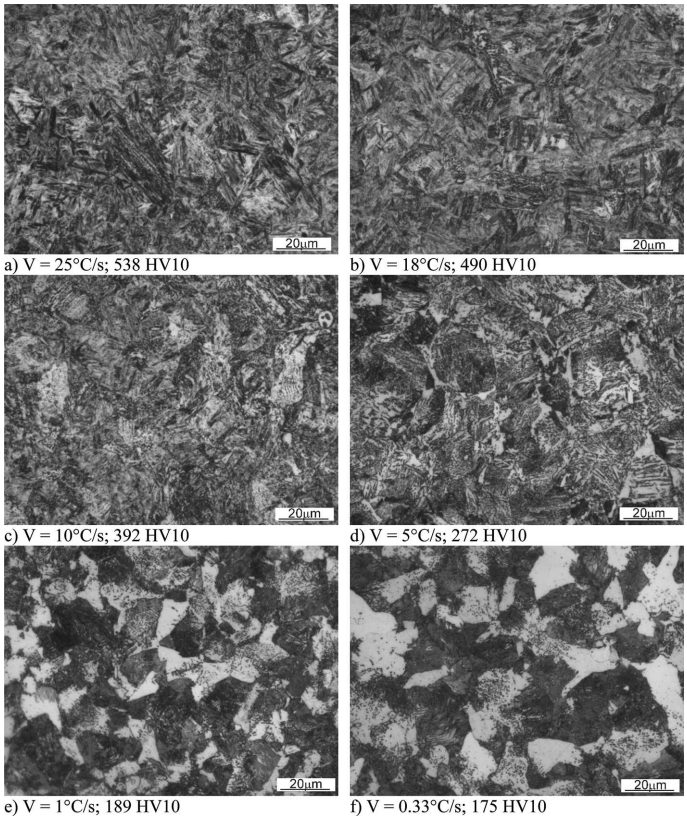

a) V = 25°C/s; 538 HV10
b) V = 18°C/s; 490 HV10
c) V = 10°C/s; 392 HV10
d) V = 5°C/s; 272 HV10
e) V = 1°C/s; 189 HV10
f) V = 0.33°C/s; 175 HV10

Fig. 7. Microstructures of dilatometric samples used for drawing of CCT diagrams of tested 38MnCrNi6-4-4 steel, austenitized at temperature T_A = 830°C [14]

Metallographic analysis of 38MnCrNi6-4-4 steel reveals that the microstructure of the sample cooled at a rate of 25°C/s is martensite with a trace of bainite (compare Fig. 7a). Within the range of the cooling rate of 18°C/s ÷5°C/s the microstructure of steel with nickel contains martensite with bainite, but there is also trace amounts of ferrite along the grain boundaries. The application of even lower cooling rates (1°C/s and 0.33°C/s) results in that the microstructure of this steel is ferrite-pearlitic one.

The microstructure of 39MnCrMo6-4-3 steel within the range of cooling rate at 50÷0.16°C/s looks similar to the one

of steel with nickel. At cooling rate of 50 and 25°C/s the microstructure of hypoeutectoid steel with molybdenum contains martensite and trace amount of bainite. Cooling at the rate of 1°C/s results in creation of distinct ferrite microstructure in Widmannstätten system. However, for the cooling rate of 0.16°C/s the microstructure of test steel is ferrite-pearlitic (compare Fig. 8f).

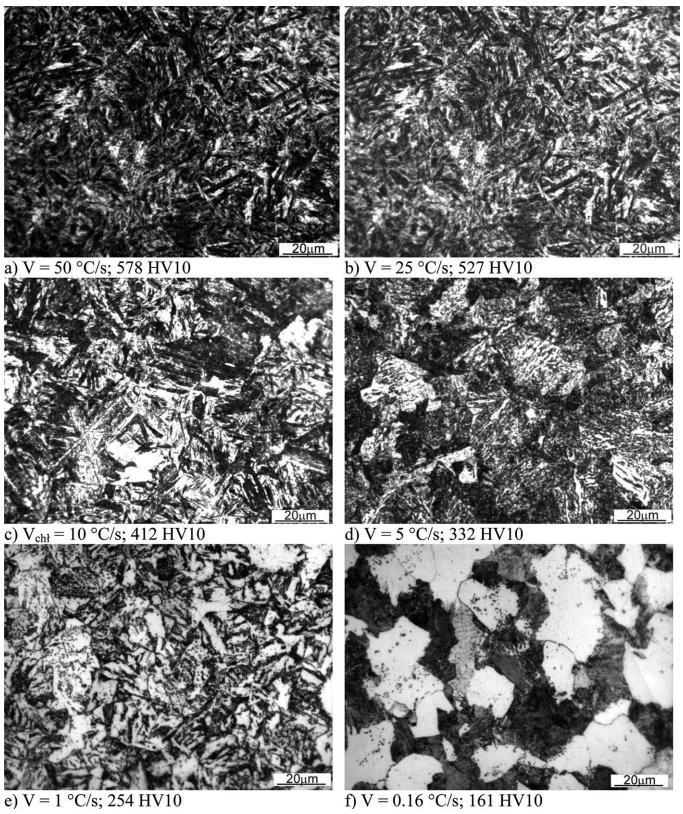

a) V = 50 °C/s; 578 HV10 b) V = 25 °C/s; 527 HV10
c) $V_{chł}$ = 10 °C/s; 412 HV10 d) V = 5 °C/s; 332 HV10
e) V = 1 °C/s; 254 HV10 f) V = 0.16 °C/s; 161 HV10

Fig. 8. Microstructures of dilatometric samples used for drawing of CCT diagrams of tested 39MnCrMo6-4-3 steel with molybdenum, austenitized at temperature T_A = 890°C

4.4. EDS analysis for two selected cooling rates of hypoeutectoid steels

Based on CCT diagrams (Fig. 5 and 6) of analyzed 38MnCrNi6-4-4 and 39MnCrMo6-4-3 steels the cooling rates were calculated directly in front of the "nose" of diffusional transformations for each of steels.

The graph (Fig. 9) presents the applied treatment methods for tested steels. A sample of steel was heated at a rate of 5°C/s and austenitized for 20 minutes (at a given T_A) and then cooled with the calculated rate in front of "nose" of diffusional transformations to a temperature below the end of the pearlitic transition, maintained for an hour and cooled at a rate of 1°C/s to room temperature.

This was followed by a point, a linear, and certain areas EDS microanalysis of tested hypoeutectoid steels. Figure 10 presents a point analysis of steel with molybdenum where there is visible higher concentration of carbon at the grain boundaries. This is probably alloyed cementite (with chrome).

In comparison with the analysis within the area of grain it can be seen that carbon in weight is about half as much (approximately 3% weight) than in case of on the grain boundaries, where the carbon is at a level of about 6% weight.

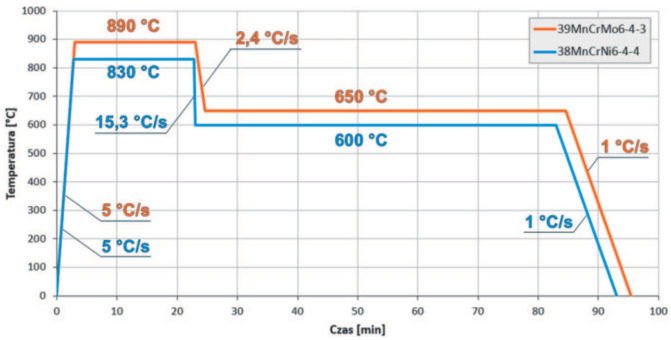

Fig. 9. The applied heat treatment with selected cooling rates for hypoeutectoid steels

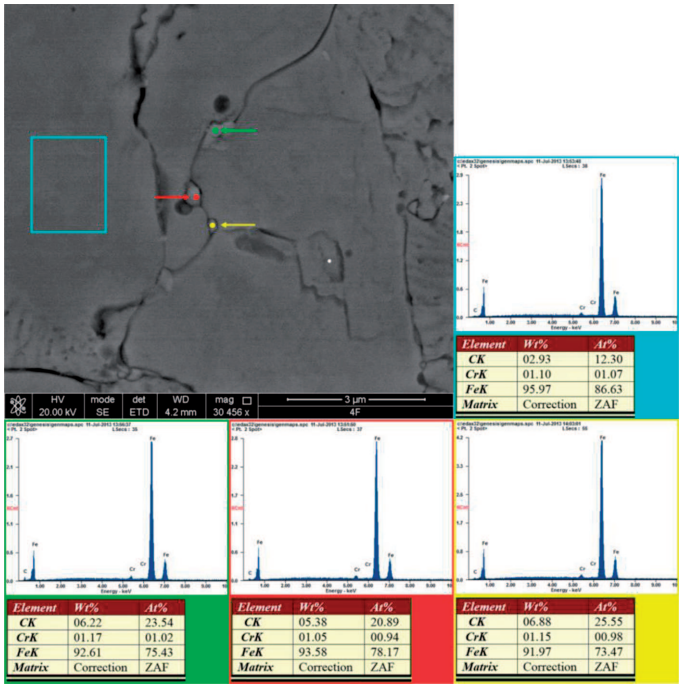

Fig. 10. Point analysis in three selected spots and grain area analysis (blue) for 39MnCrMo6-4-3 steel

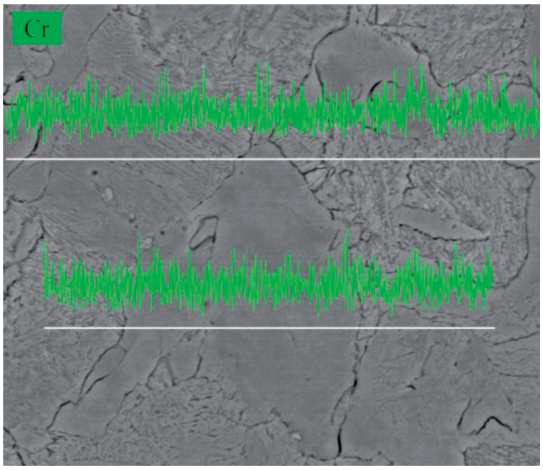

Fig. 11. Distribution of the alloying element Cr as analyzed by linear EDS for 39MnCrMo6-4-3 steel

In addition, a linear analysis of the distribution of the alloying element – Cr was performed for 39MnCrMo6-4-3 steel with molybdenum through pearlite and ferrite grains, as shown in Figure 11.

As can be seen, in both cases of the linear analysis chrome changes its concentration on the grain boundary, but in a place where probably alloyed cementite is ”built in” to the grain. This confirms the fact that carbides (especially of M_3C type) precipitate along the grain boundaries. However, in the case of transition on the pearlite/ferrite grain boundary any changes in the distribution of chromium are not observed in 39MnCrMo6-4-3steel.

Figure 12 presents an EDS point analysis of 38MnCrNi6-4-4 hypoeutectoid steel, where the increase of carbon concentration of approximately 4% weight is observed. This is most likely alloyed cementite just as in steel with molybdenum (compare Fig. 10).

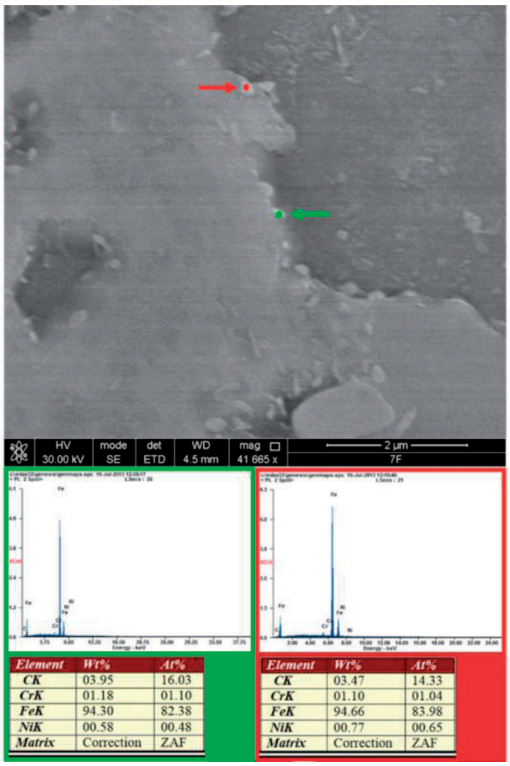

Fig. 12. EDS analysis on pearlite/ferrite grain boundary in 38MnCrNi6-4-4 steel with nickel

A similar concentration weight of carbon, but also chromium was analyzed in Figure 13, which shows an analysis of a particular area within the grains. Regardless of the morphology and the structural components present in 39MnCrMo6-4-3 hypoeutectoid steel the chemical composition remains the same.

However, in the investigated hypoeutectoid steel a linear analysis (compare Fig. 14a) showed no significant changes in the distribution of alloying elements: Cr and Ni inside the grains. Only at a magnification of 41 665x it was shown that on the pearlite / ferrite grain boundary chromium distribution changes, as well as a slight change of nickel is observed (compare Fig. 14b).

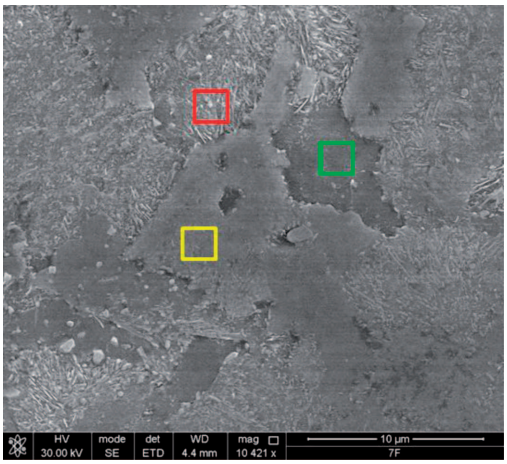

Fig. 13. EDS analysis of area within grains for 38MnCrNi6-4-4 steel

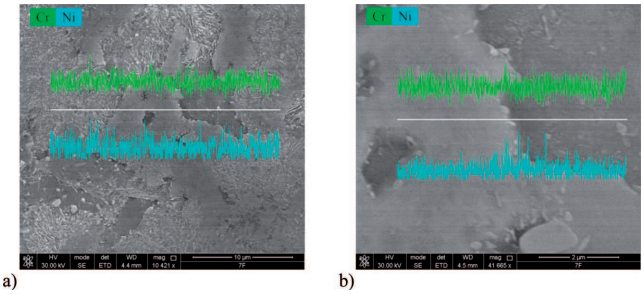

a) b)

Fig. 14. Linear EDS analysis of chrome and nickel on grain boundary for 38MnCrNi6-4-4 hypoeutectoid steel

5. Summary and conclusions

This paper presents an evaluation of the chemical composition gradients for two hypoeutectoid steels differing in alloying elements. The study included evaluation of the kinetics of phase transformations of supercooled austenite in 38MnCrNi6-4-4 and 39MnCrMo6-4-3 steels, wherein the CCT diagrams were developed for the respective austenitizing temperatures (for steel with nickel T_A = 830°C and for steel with molybdenum T_A = 890°C), which was supplemented with metallographic documentation and hardness measurements. In addition, for two selected cooling rates (before the beginning of diffusional transformations) heat treatment was performed, and EDS analysis was made (point, linear and within a specific area). This research allowed to formulate the following conclusions:

- Developed CCT diagrams in accordance with the Rose and Wever classification are of type IV, which means that the diffusional transformations are separated by a stability range of the supercooled austenite and have the shape of the letter ”C”.
- Bainite formed in both cases of examined steels was created above 350°C, which means that it is probably the upper bainite, which is dangerous because of the low resistance to cracks propagation. Upper bainite is composed of ferrite strips with precipitated cementite along grain boundaries, what significantly weakens the boundaries.
- The hardenability of tested steels is similar, but molybdenum acts much more effectively than nickel. Molybde-

num (according to J. Pacyna [16]) occupies the I-st place among the effectiveness of alloying elements for the steels designed for low tempering, where the "background" of other elements is weak.

- The austenitizing temperature of 38MnCrNi6-4-4 steel is about 60°C lower than that of 39MnCrMo6-4-3 steel. Thus, transformations of undercooled austenite were pushed towards lower temperatures, what is the direct result of nickel influence, which is an austenite creative element.
- An addition of molybdenum in amount of 0.3% results in creation of Widmannstätten microstructure when cooled at the rate of already from 1°C/s, as shown by metallographic analysis.
- For both tested hypoeutectoid steels an EDS analysis revealed the precipitation of alloyed cementite at the grain boundaries. Chromium, as a ferrite creative element, quite strongly diffuses into the grain boundaries. It is visible with the change of chromium distribution along pearlite/ferrite grains boundaries.

Acknowledgements

The author would like to thank MSc. Rafał Dziurka and PhD. Mateusz Kopyściański for their help in dilatometric investigations, EDS analysis, sugestions and advices.

REFERENCES

[1] S. Wilmes, H.J. Becker, R. Krumpholz, W. Verderber, Tool Steels. Steel, A Handbook for Materials Researched and Engineering, Springer-Verlag-Stahleisen mbH **2**, 302 (1993).

[2] R. Dąbrowski, R. Dziurka, Tempering temperature effects on hardness and impact toughness of 56NiCrMo7 steel, Archives of Metallurgy and Materials **56**, 1, 5-11 (2011).

[3] J. Pacyna, R. Dąbrowski, G. Zając, Effect of carbon content on the fracture toughness of Ni-Cr-Mo steels. Archives of Metallurgy and Materials **53**, 3, 803-808 (2008).

[4] R. Dąbrowski, J. Pacyna, J. Krawczyk, New high hardness Mn-Cr-Mo-V tool steel. Archives of Metallurgy and Materials **52**, 1, 87-92 (2007).

[5] R. Dąbrowski, E. Rożniata, R. Dziurka, The microstructures and hardness analysis of a new hypereutectoid Mn-Cr-Mo-V steel, Archives of Metallurgy and Materials **58**, 2, 563-568 (2013).

[6] J. Krawczyk, E. Rożniata, J. Pacyna, The influence of hypereutectoid cementite morphology upon fracture toughness of chromium-nickel-molybdenum cast steel, Journal of Materials Processing Technology **162-163**, 336-341 (2005).

[7] P. Bała, The kinetics of phase transformations during tempering of tool steels with different carbon content. Archives of Metallurgy and Materials **54**, 2, 491-498 (2009).

[8] E. Rożniata, R. Dziurka, J. Pacyna, The kinetics of phase transformations of undercooled austenite of the Mn-Ni iron based model alloy. Journal of Achievements in Materials and Manufacturing Engineering **49**, 2, 188-192 (2011).

[9] P. Bała, J. Pacyna, The influence of kinetics of phase transformations during tempering on high-speed steels mechanical properties. Journal of Achievements in Materials and Manufacturing Engineering **43**, 64-71 (2010).

[10] P. Bała, J. Pacyna, J. Krawczyk, The influence of the kinetics of phase transformations during tempering on the structure development in a high carbon steel. Archives of Metallurgy and Materials **52**, 1, 113-120 (2007).

[11] P. Bała, J. Pacyna, J. Krawczyk, The microstructure changes in high-speed steels during continuous heating from the as-quenched state. Kovové Materiály **49**, 2, 125-130 (2011).

[12] R. Dziurka, J. Pacyna, Influence of the carbon content on the kinetics of phase transformations during continuous heating from as-quenched state in a Cr-Mn-Mo model alloys, Archives of Metallurgy and Materials **57**, 4, 943-950 (2012).

[13] E. Rożniata, R. Dziurka, Analysis of the microstructure of 37MnMo6-3 hypoeutectoid steel, Archives of Materials Science and Engineering **58**, 2, 125-129 (2012).

[14] E. Rożniata, R. Dziurka, R. Dąbrowski, The kinetics of phase transformations of undercooled austenite of the 38MnCrNi6-4-4 hypoeutectoid steel. Journal of Achievements in Materials and Manufacturing Engineering **55**, 2, 280-284 (2012).

[15] F. Wever, A. Rose, Atlas of heat treatment of steels, Stahleien M.B.H., Düsseldorf (1961).

[16] J. Pacyna, Chemical composition and steel structures design. Faculty of Metal Engineering and Industrial Computer Science AGH, Krakow (1997) (in Polish).

Received: 20 September 2012.